Navigating the Edge: UAS Boundary Tracing for Efficient Volcanic Plume Monitoring

John Ericksen[1*], Abir Islam[1], Carter Frost[1], Kevin Aubert[4], G. Matthew Fricke[1,2]
Varsha Dani[3], Rafael Fierro[4], Tobias Fischer[5], Scott Nowicki[5], Jared Saia[1], and Melanie Moses[1,6]

***Abstract*— We present the implementation and validation of SKETCH, an algorithm that uses two Unpiloted Aerial Systems (UASs) to trace the boundary of volcanic plumes. SKETCH guarantees asymptotically optimal flight distance and turning by maintaining a *sandwich invariant* where one UAS stays inside the plume boundary (defined by a CO_2 concentration threshold) and the other UAS stays outside. The UASs adjust their flight paths based on real-time CO_2 measurements to maintain this invariant. This paper details the implementation of SKETCH on a real-world UAS platform, the Dragonfly drone. We evaluate the efficacy of SKETCH through extensive testing in physics-based simulations and real-world outdoor environments using virtual plumes. The algorithm is compared to a single-UAS baseline algorithm called ZIGZAG. Results show that SKETCH meets the expectations set by theory, and it is more efficient than ZIGZAG, achieving shorter flight paths, less turning, and faster mapping times. While ZIGZAG exhibits slightly higher accuracy in estimating plume area and boundary, SKETCH offers a more efficient real-time volcanic plume monitoring approach, especially in time-sensitive situations. These results demonstrate the feasibility and efficacy of SKETCH for real-time volcanic plume monitoring, paving the way for accurate CO_2 emission estimation in hazardous and challenging environments.**

I. INTRODUCTION

Volcanic eruptions cause widespread devastation and loss of life. Monitoring volcanic gas emissions, especially carbon dioxide (CO_2), is a crucial tool for predicting these eruptions [1]. Measuring volcanic CO_2 emissions also contributes to models of climate change [2]. We tackle this challenge by developing UASs and associated algorithms capable of efficiently mapping volcanic plumes.

Volcano gas monitoring requires safer and more efficient methods. The CO_2 plume is invisible, not co-located with visible ash plumes, and usually difficult or dangerous to access from the ground. Satellite and ground-based remote sensing of volcanic CO_2 is extremely limited [3] or relies on in situ SO_2 proxies [4], [5]. Even the most recent NASA satellite hyperspectral cameras have relatively low resolution (10 ppm of CO_2) compared in situ sensors that can be integrated into a UAS.

The VolCAN project is an interdisciplinary effort among computer scientists, geologists, and computer engineers that aims to revolutionize the study of volcanic gases using UASs. In previous field studies we have characterized volcanic CO_2 emissions in Tavurvur in Papua New Guinea [6], Tajogaite in La Palma [2], multiple eruptions in Reykjanes, Iceland [1], and CO_2 the Valles Caldera supervolcano in New Mexico, USA [7].

Fig. 1: **A UNM VolCAN Dragonfly drone flying into the plume of the actively erupting Litli-Hrtur volcano in Iceland.** This expedition involved measuring CO_2 concentrations across multiple transects of the plume to build a plume model and estimate the flux of the eruption.

We designed and field-tested the SKETCH algorithm to identify the boundary of volcanic gas plumes. We define a *plume* as the set of points with a CO_2 concentration threshold above some predetermined concentration. The *boundary* (or edge) of the plume is the polycurve containing this set of points. Finding the plume boundary is crucial since it gives both the location and cross-sectional area of the volcanic plume. SKETCH (first described in [8] and further detailed in [9]) is an efficient boundary tracing algorithm using two UASs flown in tandem. SKETCH guarantees asymptotically optimal flight distance and turning. In addition, it does not assume an unrealistically maneuverable UAS (instantaneous response time to sensor readings) , and so it is adaptable to drones with a wide range of specifications.

SKETCH operates by navigating along the boundary, maintaining a *sandwich invariant*: one UAS maintains a location with a CO_2 concentration greater than the threshold, and the other UAS maintains a location with a concentration lower than the threshold. Both move perpendicular to the concentration gradient. If a UAS crosses the boundary and the invariant is invalidated, then the UASs collaboratively turn towards the boundary to reestablish the invariant. This last step is carefully designed so that the total turning of both drones over the course of the algorithm asymptotically

[1]Department of Computer Science, University of New Mexico,[2]Center for Advanced Research Computing, University of New Mexico, [3]Computer Science Department, Rochester Institute of Technology, [4]Department of Electrical Engineering, University of New Mexico, [5]Earth and Planetary Sciences, University of New Mexico, [6]Santa Fe Institute, Santa Fe, *Correspondence: johncarl@unm.edu. This work was supported by NRI Grant 2024520.

equals the total curvature and length of the boundary.

The main contribution of this work is to demonstrate an implementation of the SKETCH algorithm in the DragonFly UAS platform; a platform that we have successfully used at multiple active eruptions. This bridges the well known and often challenging *reality gap* between theory and implementation. We validate the efficacy of SKETCH through comprehensive testing in physics-based simulations and demonstrate feasibility in UASs in real-world outdoor environments using virtual plumes, showcasing its ability to accurately trace complex plume boundaries under varying conditions. These contributions advance the state-of-the-art in collaborative UAS environmental monitoring and provide a foundation for future research and development.

II. RELATED WORK

Recent advances in UAS technology have led to significant improvements in environmental monitoring, boundary detection, and volcanic plume mapping. UASs can cover large areas, collect data from hard-to-reach places, and perform tasks with high efficiency and accuracy, and thus find applications in many domains [10]. In this section we focus on related work on environmental monitoring with UASs.

Determining the boundary of a region has many practical applications, for example: mapping pollution sources such as chemical spills and emissions [11], radiation hazards [12], agriculture [13] and volcanic plumes. Sung et al. [14] provide a survey of decision-theoretic approaches for robotic environmental monitoring.

Facinelli et al. [15] describe challenges in gas plume detection in industrial areas using coordinated UASs . Ghamry et al. [16] investigate strategies for forest monitoring and fire detection leveraging the combined capabilities of UASs and UGVs for enhanced efficiency. Additionally, Euler et al. [17] describe an adaptive sampling strategy for efficient spatial mapping in large-scale environments, through cooperative UASs. Assenine et al. [18] developed a cooperative deep reinforcement learning approach that focuses on real-time monitoring of pollution plumes using a fleet of drones equipped with advanced sensing technology. Rossi and Brunelli [19] describe a team of UASs equipped with electronic noses for effective gas detection and mapping. Karbach et al. [20] use UAS to observe volcanic plume chemistry with ultralight sensor systems. Asadzadeh et al. review [21] the state-of-the-art in UAS-based remote sensing for the petroleum industry and environmental monitoring. Saldaña et al. [22] approximate boundaries of a 2D surface oil slick using aquatic robots taking pointwise measurements.

In comparison to these earlier results which make strong assumptions on the boundary shape (e.g. convexity or star-convexity [23], [24]), our problem is both easier and harder. It's easier because we assume a largely static boundary; it's harder because we make fewer assumptions on the boundary shape. Furthermore, in contrast to most of the earlier results which use a single agent, we deploy two UASs in order to handle arbitrary boundary shapes. Rather surprisingly, the use of a UAS pair does not impact algorihmic efficiency. In fact, our theoretical results guarantee optimal distance traversed and angle turned by the UASs, while also ensuring precise estimation of the boundary. Our prior lab experiments [25] and the field experiments and simulations we present here support these theoretical guarantees.

Algorithm 1 Initially, UASs D_1, D_2 are $\sqrt{\lambda}$ apart; one inside and one outside

procedure SKETCH(λ) ▷
  $\nabla \leftarrow$ boundary gradient; SketchTerminate $\leftarrow$ **false**;
  while SketchTerminate = **false do**
    if inside (D_1) XOR inside (D_2) **then**
      Move λ distance in the direction of ∇
    end if
    if not inside (D_1) and not inside (D_2) **then**
      CROSS-BOUNDARY$(D_1, D_2, -\sqrt{\lambda})$
    elseif inside (D_1) and inside (D_2)
      CROSS-BOUNDARY $(D_2, D_1, \sqrt{\lambda})$
    end if
  end while
end procedure

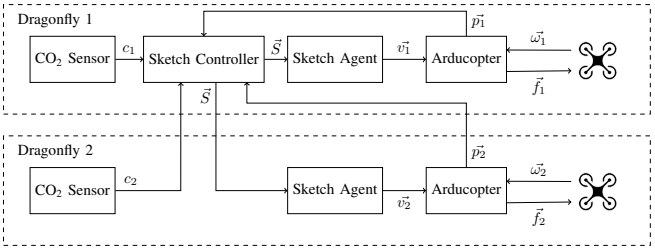

Fig. 2: **System level diagram of the Dragonfly SKETCH implementation.** The SKETCH algorithm is executed on the lead drone (Dragonfly 1) within the SKETCH Controller, which directs both itself and the follower drone's (Dragonfly 2) Sketch Agent to direct the flight path of each drone. The communication between the SKETCH Controller and the SKETCH Agents leverages the multi-agent-oriented ROS2 DDS infrastructure. Vector flight directives are issued from the SKETCH Agent to the Arducopter flight controller through the LOCAL_POSITION/VELOCITY ROS topic.

III. METHODS

A. SKETCH *Algorithm and Implementation*

We implement SKETCH (Algorithm 1; illustrated in Figure 3; see also [9] for details) with a two-level architecture depicted in Figure 2. The top level is the Sketch Controller, which runs on the leader drone (DragonFly 1 in the figure) and processes the positions and CO_2 readings from both UASs. The Sketch Controller decides whether to fly straight or turn towards the plume boundary. These decisions are sent as commands to the lower-level Sketch Agents which run on both the leader and follower drones. The Sketch Agents execute these commands, controlling the flight dynamics using velocity vector commands through the flight control computer.

The Sketch Agent flight dynamics are implemented using

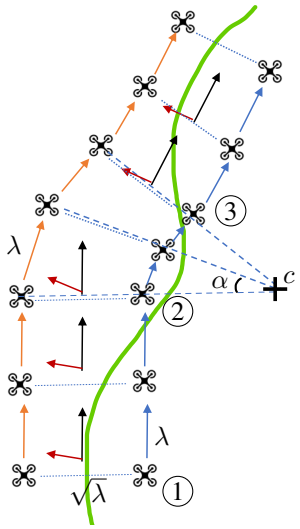

Fig. 3: **Illustration of Algorithm 1.** At ①, the UAS pair is sandwiching the edge of the plume in green. At ② a UAS has crossed the boundary, and so the UASs perform a series of turning steps to reestablish the sandwich invariant (via the CROSS-BOUNDARY subroutine). At ③ the UASs sandwich the boundary again, and so move in a straight line perpendicular to the last measured boundary gradient.

a flocking-style algorithm, which maintains alignment, cohesion, and separation between the two UASs through a linear combination of velocity vectors. The linear vector sum is given as:

$$\vec{v_i} = c_s\vec{v_s} + c_t\vec{v_t} + \Delta t(c_{to}\vec{a_{to}} + c_{ta}\vec{a_{ta}} + c_e\vec{a_e}) \quad (1)$$

In this equation:

- $\vec{v_s}$ is the straight-line velocity vector.
- $\vec{v_t}$ is the turning velocity vector.
- $\vec{a_{to}}$ is the tandem-offset acceleration vector.
- $\vec{a_{ta}}$ is the tandem-alignment acceleration vector.
- $\vec{a_e}$ is the error-correction acceleration vector.
- $\vec{\delta t}$ is the update interval in seconds for the $\vec{v_i}$ update. In our experiments $\vec{\delta t}$ is set to a constant 10 Hz.

Straight-line and turning vectors are applied based on the Sketch Controller's command vector $\vec{S}$. The constants c_s, c_t, c_{to}, c_{ta}, and c_e are gain scalars used to tune the dynamics of the algorithm.

To trace the boundary of a volcanic plume, SKETCH relies on the concept of a concentration gradient. While SKETCH assumes the gradient is provided by an oracle, in practice the gradient is calculated from readings collected along the flight paths. We evaluated several techniques for calculating the gradient, including fitting a line from three points near the plume crossing, using the previous 100 sample data points, and limiting data points to those within a distance of λ from the current position. Our results indicated that the approach of limiting data points within λ distance produced the most accurate gradient estimation compared to the oracle. This method balanced the smoothing effect by averaging multiple points while maintaining proximity to the current gradient state.

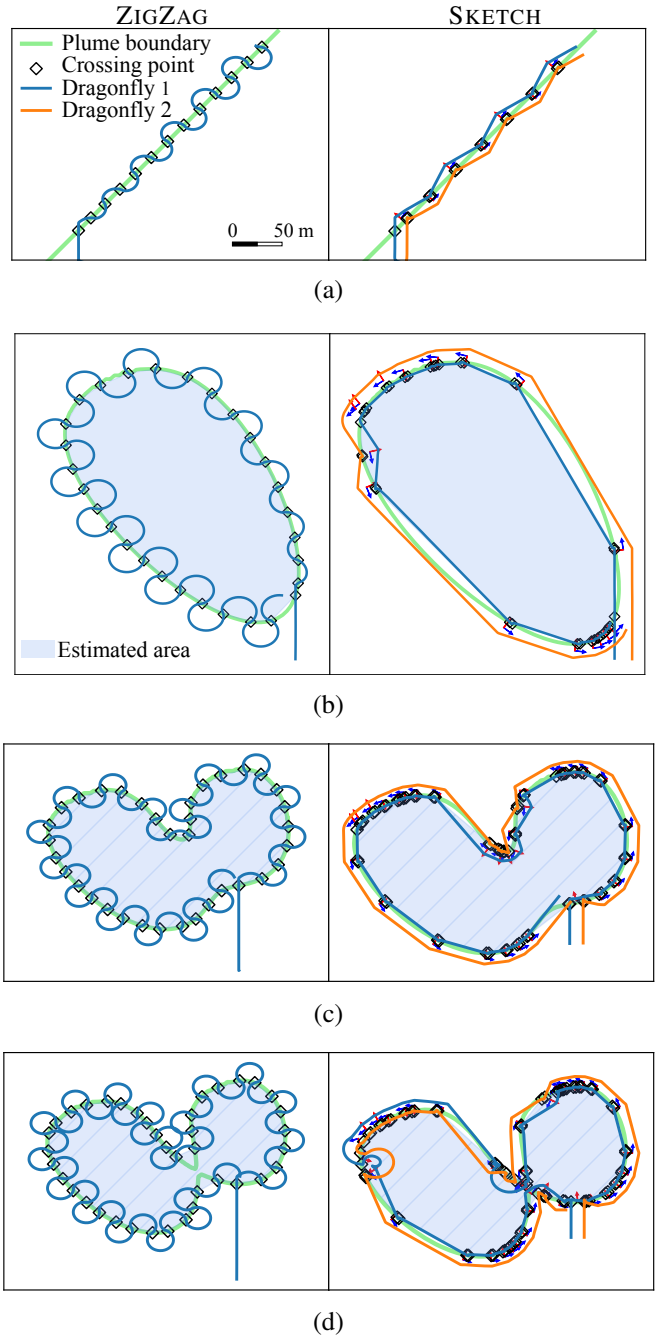

Fig. 4: **Flight path simulations of UASs executing the ZIGZAG algorithm (left) and the SKETCH algorithm (right).** Scenarios include: (a) Straight line, (b) Single plume, (c) Double plume, and (d) Dumbbell configuration. Diamond markers indicate crossing points, which are connected to estimate the plume area, shown with a hashed blue fill. Both algorithms accurately estimate plume areas, but SKETCH completes the circumnavigation 1.5 to 2 times faster.

B. ZIGZAG *Algorithm*

For comparison, we implement a single UAS boundary-following algorithm called ZIGZAG that incorporates λ that

defines the same turning behavior as SKETCH. ZIGZAG is intended to illustrate the advantages of using two UAS that maintain the sandwich invariant; it is not intended to be an optimal algorithm. ZIGZAG is conceptually similar to other line-following robot algorithms (e.g. [26]) that use sensors to determine whether a line is to the left or right of the robot. ZIGZAG turns clockwise when the robot crosses from a concentration below the boundary to one above the boundary and anticlockwise otherwise. This results in a looping path that intersects the boundary. The distance the UAS can travel from the plume is determined by the radius of the turning angle.

$$\text{ZIGZAG}(v, c, \lambda) = \begin{cases} \text{TURNRIGHT}(v, \lambda) & \text{if c} > \text{threshold} \\ \text{TURNLEFT}(v, \lambda) & \text{otherwise} \end{cases} \tag{2}$$

IV. EXPERIMENTS

To validate SKETCH, we conducted a series of experiments in both Gazebo[1] and a real-world field test. Because it is impossible to generate a large CO_2 plume at our field site, we tested SKETCH on a virtual plume simulated at the field site. This virtual plume is generated using a location-based equation based on a smeared Gaussian distribution. We conducted experiments with plumes that vary in size, shape, and CO_2 concentration gradients, providing a comprehensive assessment of the boundary-tracking capabilities of SKETCH.

To evaluated the algorithms, we focus on the following metrics: 1) Distance maintained from the plume boundary using two parameters: the Fréchet distance and the average Hausdorff distance, 2) Percent error between the ground truth plume area and the estimated area of the polygon formed by the UASs' plume-crossing points, 3) Amount of turning by the UASs, 4) UAS path length, and 5) UAS flight time. The Fréchet distance [27] measures the maximum divergence between the UAS paths and the plume boundary, assessing the worst-case separation, which is then compared to the theoretical $8\sqrt{\lambda}$ guarantee. In contrast, the average Hausdorff distance [28] measures the difference between the ground truth and the estimated plume boundary.

We simulated SKETCH and ZIGZAG in Gazebo across four cases: a straight-line threshold, a simple single-plume model, a double-plume model, and a challenging double-plume scenario with a narrow neck (dumbbell case). Finally, we conducted field tests of SKETCH using physical Dragonfly UASs capable of tracing volcanic plumes in real-world environments (Figure 5). These tests focused on validating the algorithm's performance on physical UASs. We collected data on the UASs flight paths, CO_2 readings, and their ability to track the plume under real-world conditions.

V. RESULTS

Each scenario in Gazebo was simulated once for both SKETCH and ZIGZAG, except the double-plume scenarios,

[1]Gazebo simulation: https://www.youtube.com/watch?v=-FzHBOoKdXE

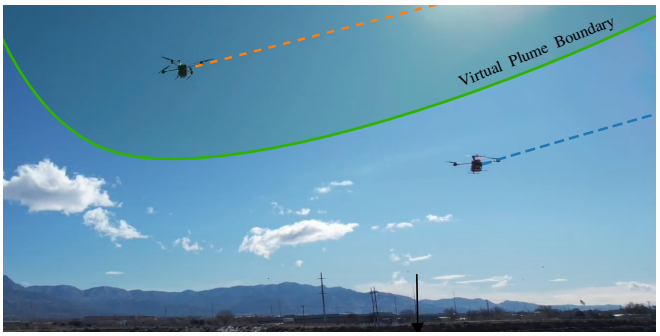

Fig. 5: **SKETCH executed using two DragonFly UAS to map a virtual plume boundary.** The pair of drones adapt their flight path to maintain the sandwich invariant.

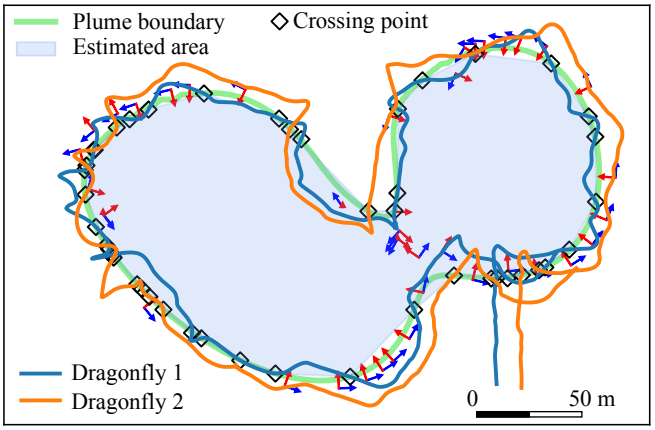

Fig. 6: **Flight paths of physical UASs executing SKETCH.** Flight paths of the Dragonfly UASs at Balloon Fiesta Park in Albuquerque, NM, showing vectors $\vec{S}$ and the total plume area. $\vec{S}$ includes the blue arrow indicating the forward or turning movement, and the red arrow indicating the calculated gradient.

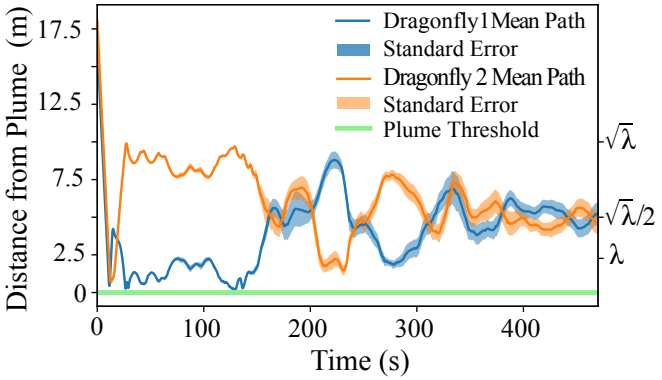

Fig. 7: **Graphical representation of the two Dragonflys' distance from the double plume threshold across 30 trials.** The distance measurements highlight the UASs' ability to consistently maintain proximity to the plume edge, with values consistently within the expected theoretical limit of $8\sqrt{\lambda}$.

TABLE I: Comparison of SKETCH and ZIGZAG.

Plume	Algorithm	Platform	Fréchet Distance (m)		Average Hausdorff Distance (m)	Plume Area Estimation Error (%)	Amount of Turning (°)		Path Length (m)		Flight Time (s)
			UAS1	UAS2			UAS1	UAS2	UAS1	UAS2	
Straight line	ZIGZAG	Gazebo	15	-	2.7	-	2400	-	400	-	260
	SKETCH	Gazebo	10	9.9	3.7	-	1400	1300	260	250	170
Single plume	ZIGZAG	Gazebo	19	-	2.5	1.2	6700	-	1100	-	760
	SKETCH	Gazebo	9.8	11	9.5	8.7	3200	1800	530	570	380
	SKETCH	Hardware	11	15	5.6	3.7	2000	1800	540	570	200
Double plume	ZIGZAG	Gazebo	18	-	2.6	2.0	8300	-	1400	-	950
	SKETCH	Gazebo	14	13	3.8	3.9	5500	4600	710	740	520
	SKETCH	Hardware	19	16	3.1	4.0	5700	5500	820	860	340
Dumbbell plume	ZIGZAG	Gazebo	19	-	2.6	3.7	10 000	-	1800	-	1200
	SKETCH	Gazebo	15	25	3.7	4.7	7000	5900	800	800	600

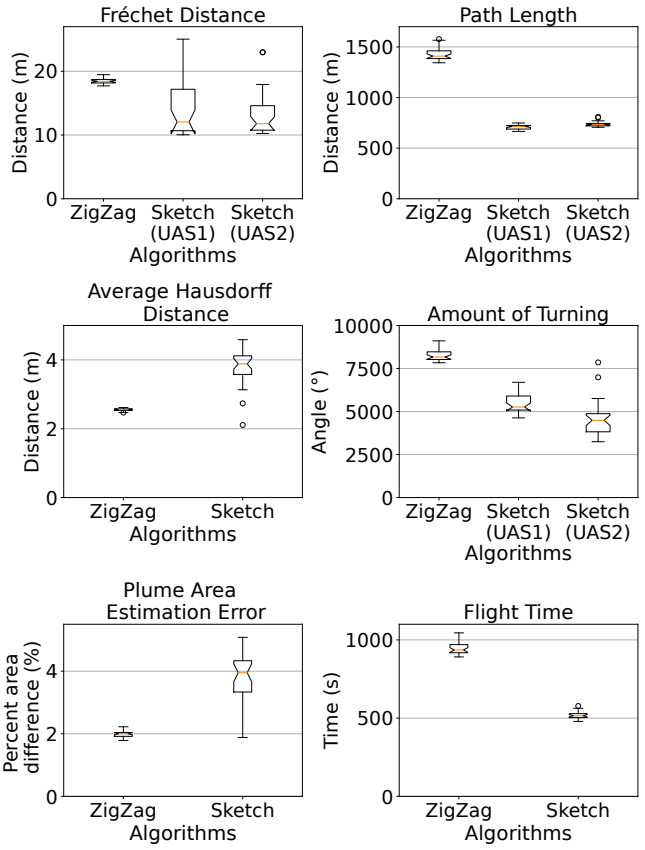

Fig. 8: **Statistical comparison between SKETCH and ZIGZAG** over 30 simulation trials on Gazebo for the double plume case. Sketch circumnavigates the plume faster due to the shorter path length with less turning. The Error introduced by the lack of interaction with the plume is minimal while the Fréchet distance from the edge of the plume is minimal and within theoretical bounds.

which were tested over 30 trials per algorithm. Furthermore, single and double-plume scenarios for SKETCH were flown using the physical Dragonfly UASs. Figure 4 displays the ground truth plume, flight paths, crossing points, and the estimated plume boundary for the Gazebo simulations of both SKETCH and ZIGZAG across the four scenarios. Meanwhile, Figure 6 presents these components for SKETCH conducted with physical Dragonfly UASs for the double plume case.

Figure 7 displays the distance from the plume boundary across 30 trials of the double plume Gazebo simulation. The UASs maintained an average distance from the boundary of $5.6\,\mathrm{m}$ with a standard deviation of $4.6\,\mathrm{m}$ and a maximum distance of $25\,\mathrm{m}$, aligning with the theoretical prediction of being within $8\sqrt{\lambda}$ (Theorem 1 in [9]), or $80\,\mathrm{m}$, where λ is a parameter that is scaled with respect to the plume having a unit diameter (see Section 1.1 in [9]). Minimizing this distance ensures that the UASs accurately traces the boundary.

Table I summarizes the performance metrics for each scenario. All values in this paper are displayed to two-significant digits. For the double plume cases, the mean values are shown in the table while a statistical comparison is presented in Figure 8 within the 30 simulation trials. In all cases, SKETCH is at least 1.5 times faster than ZIGZAG. Additionally, SKETCH demonstrates a shorter path length, lower amount of turning, and closer proximity of the UASs to the plume boundary (lower Fréchet distance), whereas ZIGZAG achieves higher accuracy in plume area and boundary estimation. The benefit of completing the map in less time is obvious in the case of mapping an active volcano. Aditionally, quadcopter turns demand more energy than straight-line flight (e.g. [29]), making reduced turning beneficial.

A class of plumes we hypothesized would be challenging for SKETCH are ones with very narrow necks [e.g. Figure 4 (d)]. These plumes have two different sections of the boundary that are within $4\sqrt{\lambda}$ of each other, which if allowed to appear arbitrarily in general shapes would make the boundary topologically degenerate and hence was ruled out as an assumption in our theoretical analysis. However, for this specific and challenging case, in practice we found that UASs executing SKETCH were able to robustly navigate the boundary.

VI. CONCLUSION

Our experiments demonstrate that SKETCH effectively navigates plume boundaries in both simulated and real-world environments. Compared to the single-UAS ZIGZAG algorithm, SKETCH demonstrates superior efficiency, achieving shorter flight paths, less turning, and faster completion times. This efficiency is crucial for real-time monitoring, especially in dynamic environments such as active volcanoes. The Dragonflies performed comparably to their simulated

counterparts in Gazebo, maintaining stable flight while accurately tracking the plume boundary. This confirms the viability of SKETCH for field deployment to estimate the area of elevated CO_2 plumes. Combined with our earlier work demonstrating flights through erupting volcanic emissions, these findings will allow scientists to efficiently estimate CO_2 plume sizes. This advancement in UAS-based plume monitoring, facilitated by SKETCH, has the potential to significantly improve the accuracy and efficiency of CO_2 emission estimation, leading to a better understanding of volcanic activity and its environmental impact.

ACKNOWLEDGMENT

JE support provided by the Department of Energys Kansas City National Security Campus, operated by Honeywell Federal Manufacturing & Technologies, LLC under contract number DE-NA0002839. GMF, SN, TF, RF, AI, JS, KA and MM support provided by the VolCAN project under National Science Foundation grant 2024520.

REFERENCES

[1] T. P. Fischer, C. L. Mandon, S. Nowicki, J. Ericksen, F. R. Vilches, M. A. Pfeffer, A. Aiuppa, M. Bitetto, A. Vitale, G. M. Fricke, M. E. Moses, and A. Stefánsson, "CO2 emissions during the 2023 Litli Hrútur eruption in Reykjanes, Iceland: 13C tracks magma degassing," *Bulletin of Volcanology*, vol. 86, no. 6, 6 2024.

[2] J. Ericksen, T. P. Fischer, G. M. Fricke, S. Nowicki, N. M. Pérez, P. Hernández Pérez, E. Padrón González, and M. E. Moses, "Drone CO2 measurements during the Tajogaite volcanic eruption," *Atmospheric Measurement Techniques*, vol. 17, no. 15, pp. 4725–4736, 8 2024. [Online]. Available: https://amt.copernicus.org/articles/17/4725/2024/

[3] W. Stremme, M. Grutter, J. Baylón, N. Taquet, A. Bezanilla, E. Plaza-Medina, B. Schiavo, C. Rivera, T. Blumenstock, and F. Hase, "Direct solar ftir measurements of co2 and hcl in the plume of popocatépetl volcano, mexico," *Frontiers in Earth Science*, vol. 11, p. 1022976, 2023.

[4] S. Carn, V. Fioletov, C. McLinden, C. Li, and N. Krotkov, "A decade of global volcanic so2 emissions measured from space, sci. rep., 7, 44095," 2017.

[5] M. S. Johnson, F. M. Schwandner, C. S. Potter, H. M. Nguyen, E. Bell, R. R. Nelson, S. Philip, and C. W. O'Dell, "Carbon Dioxide Emissions During the 2018 Kilauea Volcano Eruption Estimated Using OCO-2 Satellite Retrievals," *Geophysical Research Letters*, vol. 47, no. 24, p. e2020GL090507, 12 2020. [Online]. Available: https://agupubs.onlinelibrary.wiley.com/doi/10.1029/2020GL090507

[6] B. Galle, S. Arellano, N. Bobrowski, V. Conde, T. P. Fischer, G. Gerdes, A. Gutmann, T. Hoffmann, I. Itikarai, T. Krejci, E. J. Liu, K. Mulina, S. Nowicki, T. Richardson, J. Rüdiger, K. Wood, and J. Xu, "A multi-purpose, multi-rotor drone system for long-range and high-altitude volcanic gas plume measurements," *Atmospheric Measurement Techniques*, vol. 14, no. 6, 2021.

[7] J. Ericksen, G. M. Fricke, S. Nowicki, T. P. Fischer, J. C. Hayes, K. Rosenberger, S. R. Wolf, R. Fierro, and M. E. Moses, "Aerial Survey Robotics in Extreme Environments: Mapping Volcanic CO2 Emissions With Flocking UAVs," *Frontiers in Control Engineering*, vol. 0, p. 7, 3 2022. [Online]. Available: https://www.frontiersin.org/articles/10.3389/fcteg.2022.836720/full

[8] V. Dani, A. Islam, and J. Saia, "Boundary sketching with asymptotically optimal distance and rotation," in *International Colloquium on Structural Information and Communication Complexity (SIROCCO)*, S. Rajsbaum, A. Balliu, J. J. Daymude, and D. Olivetti, Eds. Cham: Springer Nature Switzerland, 2023, pp. 357–385.

[9] ——, "Boundary sketching with asymptotically optimal distance and rotation," *Theoretical Computer Science*, vol. 1010, p. 114714, 2024. [Online]. Available: https://www.sciencedirect.com/science/article/pii/S0304397524003311

[10] S. Javaid, N. Saeed, Z. Qadir, H. Fahim, B. He, H. Song, and M. Bilal, "Communication and control in collaborative uavs: Recent advances and future trends," *IEEE Transactions on Intelligent Transportation Systems*, 2023.

[11] M. Rossi and D. Brunelli, "Gas sensing on unmanned vehicles: Challenges and opportunities," in *Proceedings - 2017 1st New Generation of CAS, NGCAS 2017*. Institute of Electrical and Electronics Engineers Inc., 9 2017, pp. 117–120.

[12] C. Gomez and H. Purdie, "UAV- based Photogrammetry and Geocomputing for Hazards and Disaster Risk Monitoring A Review," *Geoenvironmental Disasters*, vol. 3, no. 1, pp. 1–11, 12 2016. [Online]. Available: https://link.springer.com/articles/10.1186/s40677-016-0060-yhttps://link.springer.com/article/10.1186/s40677-016-0060-y

[13] P. Radoglou-Grammatikis, P. Sarigiannidis, T. Lagkas, and I. Moscholios, "A compilation of UAV applications for precision agriculture," *Computer Networks*, vol. 172, p. 107148, 5 2020.

[14] Y. Sung, Z. Chen, J. Das, P. Tokekar *et al.*, "A survey of decision-theoretic approaches for robotic environmental monitoring," *Foundations and Trends® in Robotics*, vol. 11, no. 4, pp. 225–315, 2023.

[15] D. Facinelli, M. Larcher, D. Brunelli, and D. Fontanelli, "Cooperative uavs gas monitoring using distributed consensus," in *2019 IEEE 43rd Annual Computer Software and Applications Conference (COMPSAC)*, vol. 1. IEEE, 2019, pp. 463–468.

[16] K. A. Ghamry, M. A. Kamel, and Y. Zhang, "Cooperative forest monitoring and fire detection using a team of uavs-ugvs," in *2016 International conference on unmanned aircraft systems (ICUAS)*. IEEE, 2016, pp. 1206–1211.

[17] J. Euler, A. Horn, D. Haumann, J. Adamy, and O. Von Stryk, "Cooperative n-boundary tracking in large scale environments," in *2012 IEEE 9th International Conference on Mobile Ad-Hoc and Sensor Systems (MASS 2012)*. IEEE, 2012, pp. 1–6.

[18] M. S. Assenine, W. Bechkit, I. Mokhtari, H. Rivano, and K. Benatchba, "Cooperative deep reinforcement learning for dynamic pollution plume monitoring using a drone fleet," *IEEE Internet of Things Journal*, 2023.

[19] M. Rossi and D. Brunelli, "Autonomous gas detection and mapping with unmanned aerial vehicles," *IEEE Transactions on Instrumentation and measurement*, vol. 65, no. 4, pp. 765–775, 2015.

[20] N. Karbach, N. Bobrowski, and T. Hoffmann, "Observing volcanoes with drones: studies of volcanic plume chemistry with ultralight sensor systems," *Scientific reports*, vol. 12, no. 1, p. 17890, 2022.

[21] S. Asadzadeh, W. J. de Oliveira, and C. R. de Souza Filho, "Uav-based remote sensing for the petroleum industry and environmental monitoring: State-of-the-art and perspectives," *Journal of Petroleum Science and Engineering*, vol. 208, pp. 1–14, 2022.

[22] D. Saldaña, R. Assunção, M. A. Hsieh, M. F. Campos, and V. Kumar, "Estimating boundary dynamics using robotic sensor networks with pointwise measurements," *Autonomous Robots*, vol. 45, pp. 193–208, 2021.

[23] C. R. Heckman, I. B. Schwartz, and M. A. Hsieh, "Toward efficient navigation in uncertain gyre-like flows," *The International Journal of Robotics Research*, vol. 34, no. 13, pp. 1590–1603, 2015. [Online]. Available: https://doi.org/10.1177/0278364915585396

[24] A. Jahn, R. J. Alitappeh, D. Saldaa, L. C. A. Pimenta, A. G. Santos, and M. F. M. Campos, "Distributed multi-robot coordination for dynamic perimeter surveillance in uncertain environments," in *2017 IEEE International Conference on Robotics and Automation (ICRA)*, 2017, pp. 273–278.

[25] J. Ericksen, K. Aubert, A. Islam, G. M. Fricke, V. Dani, R. Fierro, T. P. Fischer, S. Nowicki, J. Saia, and M. Moses, "From proof to practice: Asymptotically optimal boundary mapping by two robots," *Contributed Paper*, September 2024, submitted on September 13, 2024.

[26] R. A. Schmidt Jr, *A study of the real-time control of a computer-driven vehicle*. Stanford University, 1971.

[27] H. Alt and M. Godau, "Computing the fréchet distance between two polygonal curves," *International Journal of Computational Geometry & Applications*, vol. 5, no. 01n02, pp. 75–91, 1995.

[28] A. A. Taha and A. Hanbury, "An efficient algorithm for calculating the exact hausdorff distance," *IEEE transactions on pattern analysis and machine intelligence*, vol. 37, no. 11, pp. 2153–2163, 2015.

[29] A. Nguyen, D. Krupke, M. Burbage, S. Bhatnagar, S. P. Fekete, and A. T. Becker, "U sing a uav for destructive surveys of mosquito population," in *2018 IEEE International Conference on Robotics and Automation (ICRA)*. IEEE, 2018, pp. 7812–7819.